Strain-controlled anisotropic electronic transport in $Bi_{0.4}Ca_{0.6}MnO_3$ films

Y. Z. Chen, J. R. Sun,[a] S. Liang, W. M. Lu, and B. G. Shen
Beijing National Laboratory for Condensed Matter Physics and Institute of Physics, Chinese Academic of Sciences, Beijing 100190, People's Republic of China

(Received 2 July 2008; accepted 19 October 2008; published online 9 December 2008)

Structural and resistive anisotropy has been studied for the $Bi_{0.4}Ca_{0.6}MnO_3$ films grown on (011)-oriented $SrTiO_3$ substrates. Strong anisotropic transport behaviors are observed when significant lattice strains exist. The ratio of the two resistivities along the *a* and *c* axes of the films can be tuned between ~1 and ~13 by adjusting the a/c ratio between ~1.01 and ~1.04, which can be conducted simply by decreasing film thickness from 100 to 10 nm. Considerable anisotropy emerges and develops when film thickness drops below ~60 nm. With the decrease in film thickness, a change in preferred growth direction of the films is also observed. These features of the lattice effects could be useful for the design of artificial materials and devices. © *2008 American Institute of Physics*. [DOI: 10.1063/1.3035914]

An important feature of perovskite manganites is the coexistence of strongly coupled spin, charge, and orbital degrees of freedom.[1] The ordering-disordering transition associated with either of these degrees of freedom can result in dramatic effects. A typical example is the appearance of significant magnetic and resistive anisotropies accompanying the spin and orbital ordering. It has been reported that, associated with the ferromagnetic (FM) aligning of spins in the *a-b* plane in $Nd_{0.45}Sr_{0.55}MnO_3$, a metallic conduction appears in the *a-b* plane, though semiconducting behavior remains along the *c* direction, and the resistivity in the *c* axis can be two orders of magnitude larger than that in the *a-b* plane.[2] Therefore, the anisotropic magnetic and resistive behaviors can provide valuable information on the configurations of spins, charges, and orbitals in the manganites.

For ordinary bulk manganites, however, anisotropy is usually unobvious because of the high structural symmetry and did not get much attention in the past decade. In contrast, the crystal structure of manganite films can be considerably modified by lattice strains imposed by substrates, which is expected to affect the physical properties of the films. Therefore, it is possible for the double exchange among Mn ions to be modulated by the lattice distortions that affect the spatial orientation of electron orbitals, thus the Mn 3*d* and O 2*p* overlap. As reported, the magnetic ordering of the $La_{1-x}Sr_xMnO_3$ films can be either FM or antiferromagnetic (AF), and the spin structures of the AF state are completely different, varying from A-type to CE-type and G-type successively as lattice strain is enhanced.[3] There is also evidence for preferred orbital occupancy caused by lattice strain or interface.[4,5] These results indicate that strain controlling could be an effective approach to manipulate the physical properties of the manganites.

Variant structure deformations have been obtained by selecting appropriate substrates that have different lattice mismatches with the films and different crystal orientations, and much work has been done to elucidate the lattice effects thus resulted. However, investigations on the anisotropic transport property of the films are relatively limited. An important reason may be the difficulty for the measurements of the resistivities along different directions, especially when a (100)-orientated substrate is adopted.[6] Fortunately, direction-dependent lattice strains within the film plane can be induced by (011)-orientated substrates, which yield anisotropic in-plane behaviors.[7] In this case, the resistivities along two different directions [100] and [0–11] can be conveniently determined.[8]

Noting the fact that thin films are involved in most of the artificial materials and devices, it is important to perform a thorough exploration of the lattice effects and clarify how far the physical property of the films can go under the impact of lattice strains. Based on this consideration, here we will present a systematic study on the strain-controlled anisotropic electronic transport behaviors in the $Bi_{0.4}Ca_{0.6}MnO_3$ films. Tunable, yet strong, anisotropic conductions are observed in the films grown on (011)-orientated $SrTiO_3$ substrates. The ratio of the two resistivities along the *a* and *c* axes, respectively, varies between 1 and 13, increasing as film thickness decreases. A systematic evolution of the surface morphology of the films is also observed with the relaxation of lattice strains.

$Bi_{0.4}Ca_{0.6}MnO_3$ (BCMO) films with the thickness of 10–200 nm were prepared on (011)-oriented $SrTiO_3$ substrates by the pulsed laser ablation technique. Detailed procedures for sample preparation can be found elsewhere.[9] The structural properties of the films were analyzed by x-ray diffraction (XRD) performed on a Philips X'pert Pro diffractometer at the ambient temperature. Surface morphology was analyzed by an atomic force microscopy (AFM). Resistivities along the [100] and [0–11] directions of the films, respectively, were measured by a physical property measurement system (PPMS-14h) for bridge-shaped samples (0.1 mm in width and 0.4 mm in length) using the four-probe method. The samples were patterned by the conventional photolithography and chemical etching technique.

As shown by the AFM analyses, the strained ultrathin film, for example, $t=10$ nm, exhibits a three-dimensional

[a]Author to whom correspondence should be addressed. Electronic mail: jrsun@g203.iphy.ac.cn.

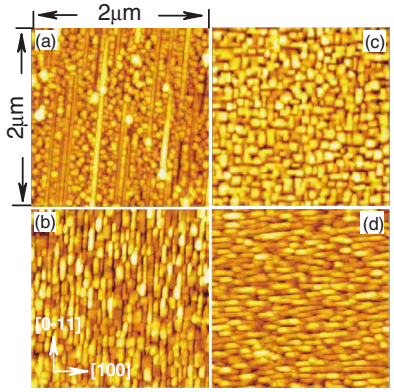

FIG. 1. (Color online) Surface morphology of the BCMO films measured by atomic force microscope. The film thicknesses are (a) 10 nm, (b) 40 nm, (c) 60 nm, and (d) 100 nm.

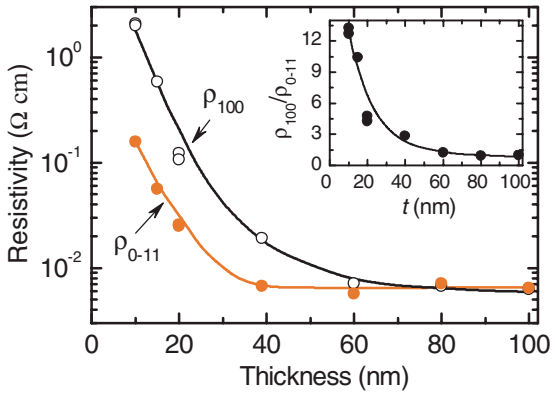

FIG. 3. (Color online) Thickness-dependent resistivities at the ambient temperature measured along the [100] and [0–11] directions, respectively. The inset plot shows the ρ_{100}/ρ_{0-11} ratio as a function of film thickness. The solid lines are guides for the eye.

island growth, with a few [0–11]-oriented stripes above the background of island-shaped grains (Fig. 1), which indicates the presence of a preferred coalescence of islands along the [0–11] direction. As film thickness increases, the [0–11] stripes become shorter and broader, forming rectangular grains (t=40 nm in Fig. 1). Unexpectedly, a reorientation of the rectangular stripes from the [0–11] direction toward the [100] direction occurs when t exceeds ~80 nm and well [100]-aligned stripes are formed in the film of 100 nm. In the intermediate thickness range, mosaic-shaped grains dominate the morphology of the film. These results reveal the difference in preferred growth directions for strained and relaxed films.

Figure 2 shows the temperature-dependent resistivity along the [100] and [0–11] axes (ρ_{100} and ρ_{0-11}) for the films with thicknesses of 10, 40, and 100 nm. Semiconductive behaviors characterized by the rapid increase in resistivity upon cooling occur in all of the films. A general tendency to highly

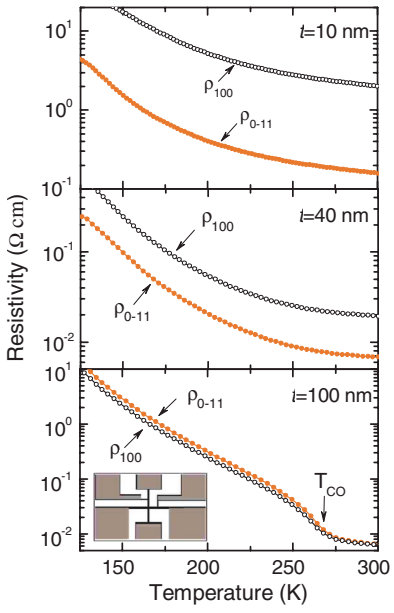

FIG. 2. (Color online) Temperature-dependent resistivities of the BCMO films with different thicknesses measured along the [100] and [0–11] axes, respectively. The inset plot is a schematic of the patterned sample. T_{CO} marks the critical temperature of charge ordering transition.

resistive states is observed as film thickness decreases, especially when t is lower than 40 nm. The most remarkable result is the appearance of a strong electronic anisotropy accompanying the resistivity enhancement: the resistivities in the [100] and [0–11] directions are rather different. This feature is unobvious in thick films (t>80 nm), for which ρ_{0-11} is a little larger than ρ_{100} both above and below T_{CO} (T_{CO} is the critical temperature for charge ordering transition). However, ρ_{100} grows rapidly with the decrease in the film thickness and exceeds ρ_{0-11} greatly when $t \leq 40$ nm. It should be noted that the $\ln \rho_{100}-T$ and $\ln \rho_{0-11}-T$ curves are approximately parallel with each other when films are thin, which is indicative of the temperature independence of ρ_{100}/ρ_{0-11}. In addition, the ρ_{100}/ρ_{0-11} exhibits slight temperature dependence as t>60 nm due to the preferential occupation of e_g orbitals accompanying the charge ordering transition. In contrast to the slight temperature-dependent anisotropy, the large transport anisotropy with decreasing film thickness is a much more apparent phenomenon.

Figure 3 illustrates the variations in ρ_{100} and ρ_{0-11} against film thickness at a fixed temperature of 300 K. It shows the clear tendency of resistivity enhancement with decreasing t. This process evolves differently in the two directions. Considerable resistive increase begins at $t \approx 70$ nm for ρ_{100} and $t \approx 50$ nm for ρ_{0-11}, respectively, which indicates an anisotropic thickness dependence of the resistivity. Strong electronic anisotropy appears at $t \approx 50$ nm and develops rapidly as t further decreases (inset in Fig. 3). A simple estimate shows that ρ_{100}/ρ_{0-11} is ~1.24 for t=60 nm and ~13 for t=10 nm. A nearly exponential increase in the ρ_{100}/ρ_{0-11} ratio with the decrease in t, $\rho_{100}/\rho_{01-1} \approx 19.68 \exp(-0.0469t)$, is observed for t<60 nm. According to this relation, the utmost ρ_{100}/ρ_{0-11} ratio will be ~20 in the thin film limit of $t \rightarrow 0$, which approximates to the anisotropy in the $La_{1.2}Sr_{1.8}Mn_2O_7$ bilayer.[8] The failure of the exponential relation in the films thicker than 80 nm may be a consequence of strain relaxation, the effects of which could be strong in thick films noting the emergence of the charge ordering transition.[10]

It has been demonstrated that the disappearance of clear charge ordering transition at t<60 nm results from the

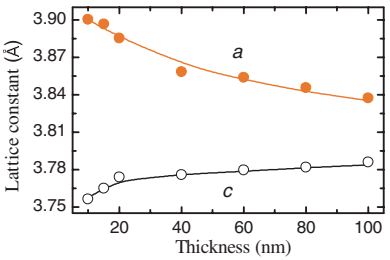

FIG. 4. (Color online) Lattice constants a and c of the BCMO films as functions of film thickness obtained at the ambient temperature. The solid lines are guides for the eye.

strain-induced lattice distortions.[10] Here, the obvious thickness-dependent transport anisotropy may have the same origin since the lattice distortions that influence the Mn $3d$ and O $2p$ overlap is expected to affect the double exchange among Mn ions, thus the physical properties of the manganites.[3] To get the information on structural distortions, XRD spectra of the (001) and (011) planes of the films are measured. The XRD data reveal a complete clamping of the [100] axis by the substrate while a partial relaxation of the [0–11] axis in the film of 10 nm. A gradual relaxation of lattice strains appears with the increase in the film thickness. It proceeds more rapidly in the [0–11] direction than in the [100] direction and remains considerable up to the thickness of 100 nm. With the assumption of $b \approx c$ (without charge ordering), the lattice constants a, b, and c can be derived from the XRD data as shown in Fig. 4, and a simple calculation gives the largest changes in lattice constants of $\Delta a/a \approx 1.62\%$ and $\Delta c/c \approx 0.81\%$ as film thickness grows from 10 to 100 nm.

Considering the fact that the crystal structure of the BCMO film is nearly orthorhombic, ρ_{0-11} can be expressed in terms of ρ_{001} and ρ_{010} through the relation of $\rho_{0-11} = \rho_{010} \sin^2 \theta + \rho_{001} \cos^2 \theta$, where $\theta \approx 45°$ is the angle between the [001] and [0–11] axes. With the assumption of $\rho_{0-11} \approx \rho_{011}$, we obtain $\rho_{0-11} \approx \rho_{010} \approx \rho_{001}$. This result means that $\rho_{100}/\rho_{0-11} \approx \rho_{100}/\rho_{001}$, that is, the observed anisotropy is actually the resistivity difference between a and c axes.

It is obvious that when lattice constant expands along one of the axes of the unit cell, the orbital overlap of the $3d$ and $2p$ electrons will reduce in this direction, leading to the increased resistivity. Furthermore, the anisotropy nature of the $3d$ orbitals may lead to anisotropic electronic transport. Figure 5 exemplifies the variation in ρ_{100}/ρ_{001} with a/c. Data of $Bi_{0.53}Sr_{0.47}MnO_3$ (BSMO),[11] $La_{0.93}Sr_{0.07}MnO_3$ (LSMO),[12] $Nd_{0.5}Sr_{0.5}MnO_3$,[13,14] and $Nd_{0.45}Sr_{0.55}MnO_3$ (Ref. 2) are also presented for comparison. According to Fig. 5, the ρ_{100}/ρ_{001} ratio is essentially unaffected when lattice strains are small ($a/c < 1.02$) and linearly grows with a/c at a rate of ~658.4 when the latter exceeds ~1.02. It seems that the $\rho_{100}/\rho_{001} - a/c$ relation is universal. The data of BSMO, LSMO, and $Nd_{0.5}Sr_{0.5}MnO_3$ also locate at this curve, though the manganites and their states are quite different. The former two compounds are in the charge-ordered state at the ambient temperature, and the third one is charge-ordered or charge-disordered below or above ~150 K. The $\rho_{100}/\rho_{001} - a/c$ dependence in $Nd_{0.45}Sr_{0.55}MnO_3$, which is in temperature

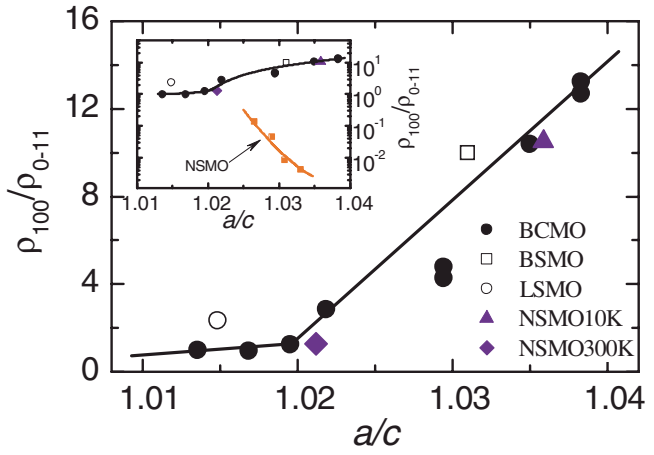

FIG. 5. (Color online) Variation in the ρ_{100}/ρ_{001} ratio with lattice strains that are characterized by a/c. Data of $Bi_{0.53}Sr_{0.47}MnO_3$ at 300 K (BSMO), $La_{0.93}Sr_{0.07}MnO_3$ at 300 K (LSMO), and $Nd_{0.5}Sr_{0.5}MnO_3$ at 10 K (NSMO10K) and 300 K (NSMO300K) are also presented for comparison. The inset plot is the same relation plotted in semilog scale with the added data of $Nd_{0.45}Sr_{0.55}MnO_3$ in the AF state (NSMO). The solid lines are guides for the eye.

range below the AF transition, is completely different, and the anisotropy is much strong compared with other manganites with the same a/c ratios (inset in Fig. 5). This is a consequence of the FM ordering in the a-b plane and the AF ordering between planes. Two conclusions can be drawn from these results. The first one is that the ρ_{100}/ρ_{001} ratio can be tuned in a wide range simply by changing lattice strains and the second one is that the electronic anisotropy in the manganites may have the same origin except when spins order along the preferred directions.

Electronic anisotropy is generally weak in bulk manganites because of the high structural symmetry. Considerable anisotropy appears only when structural transition occurs, accompanying with either a charge/orbital ordering or a spin ordering. However, the anisotropy in that case cannot be controlled. In addition to revealing the strong lattice effects, the present work provides a powerful approach to continuously tune the electronic anisotropy in a wide range simply by adjusting the lattice strains in the films. This result could be useful for the designing of artificial materials and devices.

In summary, structural and resistive anisotropy has been studied for the $Bi_{0.4}Ca_{0.6}MnO_3$ films grown on (011)-oriented $SrTiO_3$ substrates. Strong anisotropic transport behaviors are observed when significant lattice strains exist. The ratio of the two resistivities along the a and c axes of the films can be tuned between ~1 and ~13 by adjusting the a/c ratio between ~1.01 and ~1.04, which can be conducted simply by decreasing film thickness from 100 to 10 nm. Considerable anisotropy emerges and develops when film thickness drops below ~60 nm. With the decrease in film thickness, a change in the preferred growth direction of the films is also observed. This may be a result of strain relaxation. These features of the lattice effects could be useful for the designing of artificial materials and devices.

This work has been supported by the National Natural

Science Foundation of China, the National Basic Research of China, and the Knowledge Innovation Project of the Chinese Academy of Sciences.

[1]*Colossal Magnetoresistive Oxides*, edited by Y. Tokura (Gordon and Breach, London, 1999).
[2]H. Kuwahara, T. Okuda, Y. Tomioka, A. Asamitsu, and Y. Tokura, Phys. Rev. Lett. **82**, 4316 (1999).
[3]Z. Fang, I. V. Solovyev, and K. Terakura, Phys. Rev. Lett. **84**, 3169 (2000).
[4]A. Tebano, C. Aruta, S. Sanna, P. G. Medaglia, G. Balestrino, A. A. Sidorenko, R. De Renzi, G. Ghiringhelli, L. Braicovich, V. Bisogni, and N. B. Brookes, Phys. Rev. Lett. **100**, 137401 (2008).
[5]L. Abad, V. Laukhin, S. Valencia, A. Gaup, W. Gudat, L. Balcells, and B. Martinez, Adv. Funct. Mater. **17**, 3918 (2007).
[6]J. Klein, J. B. Philipp, D. Reisinger, M. Opel, A. Marx, A. Erb, L. Alff, and R. Gross, J. Appl. Phys. **93**, 7373 (2003).
[7]I. C. Infante, J. O. Osso, F. Sanchez, and J. Fontcuberta, Appl. Phys. Lett. **92**, 012508 (2008).
[8]Y. Takamura, J. K. Grepstad, R. V. Chopdekar, Y. Suzuki, A. F. Marshall, H. Zheng, and J. F. Mitchell, Appl. Phys. Lett. **87**, 142508 (2005).
[9]Y. Z. Chen, J. R. Sun, D. J. Wang, S. Liang, J. Z. Wang, Y. N. Han, B. S. Han, and B. G. Shen, J. Phys.: Condens. Matter **19**, 442001 (2007).
[10]Y. Z. Chen, J. R. Sun, S. Liang, W. M. Lu, B. G. Shen, and W. B. Wu, J. Appl. Phys. **103**, 096105 (2008).
[11]K. Taniguchi, S. Nishiyama, T. Arima, S. Konno, S. Yamada, and E. Sugano, Appl. Phys. Lett. **90**, 153501 (2007).
[12]N. I. Solin, V. A. Kazantsev, L. D. Fal'kovsaya, and S. V. Naumov, Phys. Solid State **47**, 1900 (2005).
[13]Y. Ogimoto, M. Nakamura, N. Takubo, H. Tamaru, M. Izumi, and K. Miyano, Phys. Rev. B **71**, 060403 (2005).
[14]Y. Wakabayashi, D. Bizen, Y. Kubo, H. Nakao, Y. Murakami, M. Nakamura, Y. Ogimoto, K. Miyano, and H. Sawa, J. Phys. Soc. Jpn. **77**, 014712 (2008).